Large–scale shell model calculations for ^{140}Xe

Sevdalina Dimitrova[1] and *Nicola* Lo Iudice[2,3]

[1]Institute of Nuclear Research and Nuclear Energy, Bulgarian Academy of Sciences, 1784 Sofia, Bulgaria
[2]Dipartimento di Fisica, Università di Napoli Federico II, Monte S. Angelo, via Cintia, I-80126 Napoli, Italy
[3]Istituto Nazionale di Fisica Nucleare, Sezione di Napoli, Monte S. Angelo, via Cintia, I-80126 Napoli, Italy

Abstract. This paper presents the results of a large–scale shell model calculations of the yrast spectrum of ^{140}Xe. We extend the previous calculations confined to low-lying angular momenta to high-spin states applying the same importance sampling iterative matrix diagonalization algorithm. Excitation energies and transition probabilities are obtained by using an effective nucleon–nucleon interaction derived from the CD-Bonn nucleon-nucleon potential. A satisfactory agreement with the experimental data and the previous results for low lying states is achieved.

1 Introduction

The interplay of nuclear collectivity and shell effects is an interesting phenomenon, which is intensively studied both theoretically and experimentally. Spectroscopic measurements on several chains of nuclei including Te, Xe, Ba, and Ce isotopes [1] have been supported by theoretical investigations carried out within the quasiparticle-phonon model (QPM) (see [2] for references), large–scale shell model [3–7], and in the nucleon pair approximation [8].

All theoretical studies were focused mainly on the quadrupole collectivity of the lowest isoscalar and mixed symmetry 2^+ states and therefore treated only low-lying levels of low spin. We intend to explore the possibility of extending the description of the spectroscopic properties of the nuclei in this region by computing the levels of higher spins. The Te and Xe isotopic chains have been studied already within a shell model approach endowed with an importance sampling [9] using the CD-Bonn two-body potential in a large configuration space [7]. The calculations were confined to the levels of spin up to $J^\pi = 6^+$.

In this paper our attention will be concentrated on the neutron-rich ^{140}Xe isotope. The first results for ^{138}Xe have been reported in [10]. We adopt the same approach to investigate the spectroscopic properties of the yrast line of ^{140}Xe up to $J^\pi = 12^+$.

After a brief description of the algorithm we analyze the results by relating them to the available experimental data.

2 The algorithm

The algorithm we use for the present large-scale shell model calculations is described in [9, 11]. Here we will sketch briefly the main steps of the procedure.

Let us consider a symmetric matrix representing a self-adjoint operator $\hat{A}$ in an orthonormal basis $\{|\,1\rangle, |\,2\rangle, \ldots, |\,N\rangle\}$. In order to determine the lowest m eigenvectors of the matrix we have to follow an initialization loop and a subsequent set of refinement loops.

The initialization loop:

• The initialization begins by diagonalizing the matrix (a_{ij}) $(\mathrm{i,j} = 1, \mathrm{n})$, where n fulfills the relation $(m < n' \ll N)$.

• We choose the lowest m eigenvalues λ_i and eigenvectors $|\,\phi_i\rangle$ and construct a new matrix of dimensions $(m + n')$.

$$\alpha = \begin{pmatrix} \lambda & b_j \\ b_j & a' \end{pmatrix} \quad , \tag{1}$$

where $\{\lambda\}$ is a diagonal block composed of the eigenvalues $(\lambda_i^{n'}, i = 1, m)$, a' is the new submatrix $a'_{jj'} = \langle j \mid \hat{A} \mid j' \rangle$ with $(j, j' = n + 1, n')$, and $\{b_j\}$ is an off-diagonal block connecting λ to a and is composed of the elements $b_{ij} = \langle\, \phi_i^n \mid \hat{A} \mid j \,\rangle$ where $(i = 1, m;\ j = n + 1, n')$.

• We add the lowest m eigenvalues $\lambda_i^{n'}$ together with the corresponding eigenvectors $|\,\phi_i^{n'}\rangle$ to a new subset of orthonormal states $|\,j\rangle$ to build a new matrix and proceed as we did for α.

This initialization loop ends when the whole configuration space is exhausted. As a result, a zero order approximation to the lowest eigenvalues and eigenvectors is obtained

$$E_i^{(0)} \equiv \lambda_i^N, \quad |\,\psi_i^{(0)}\rangle \equiv |\,\phi_i^N\rangle = \sum_{j=1}^{N} c_j^{(N)} \mid j\rangle \ , \quad \{i = 1, m\}. \tag{2}$$

The refinement loop:

The solutions of the eigenvalue Eqs. (2) are used as an entry to the first refinement loop, which goes through the

same steps as described above with one difference. One should just solve an eigenvalue problem of general form since the vectors $|\phi\rangle$ and $|j\rangle$ are no longer orthogonal. It has been shown in [9] that the eigenvalues $E^{(n)}$ and eigenvectors $|\psi^{(n)}\rangle$ obtained after the n-th loop converge to the solution of the exact diagonalization of $\langle\hat{A}\rangle$.

The importance sampling:

The implementation of the method requires an adequate sampling criterion for reducing the size of the configuration space. Bearing in mind that the algorithm provides accurate solutions already after the initialization loop, one can sample the configuration space as follows:

• Diagonalize the submatrix $\{a_{ij}\}(i,j=1,m)$ and obtain its eigenvalues λ_i;

• For $j=m+1,\ldots,N$, diagonalize the $m+1$-dimensional matrix

$$\alpha = \begin{pmatrix} \Lambda_m & \vec{b}_j \\ \vec{b}_j^T & a_{jj} \end{pmatrix}, \qquad (3)$$

where $\vec{b}_j = \{b_{1j}, b_{2j}, \cdot, b_{mj}\}$.

• Accept the new state only if

$$\sum_{i=1,m} |\lambda_i' - \lambda_i| > \epsilon \quad , \qquad (4)$$

otherwise ignore the state and continue the sampling process with a new vector j. In the relation above ϵ is a small parameter which allows to control the accuracy of the truncation. In the actual calculations we use an upgraded important sampling procedure [12, 13].

The algorithm outlined above contains the two key elements, the diagonalization procedure and the importance sampling, which are closely related. Thy ensure a robust and always ghost–free solutions. Moreover, the accuracy of the truncation procedure is fully under control.

3 Shell model calculations

We will keep the details of our calculations unchanged as reported in [10]. The nucleus ^{140}Xe is considered as a ^{132}Sn core plus four valence protons in the $(1g_{7/2},d_{5/2},2d_{3/2},1h_{11/2},3s_{1/2})$ model space and four valence neutrons occupying the $(2f_{7/2},3p_{3/2},1h_{9/2},3p_{1/2},2f_{5/2},1i_{13/2})$ levels. The single-particle energies are the same as in [7, 10]. They are listed in Table 1.

The effective two–body potential is a renormalized G matrix [14] derived from the CD–Bonn potential [15]. As in the previous calculations [7, 10] scaling factors for the pairing-like components of the two–body potential were adopted. We will scale just the proton–proton $J^\pi = 0^+$ components by the factor of 0.85 as we find it optimal for reproducing the experimental values of the excitation levels up to $J^\pi = 12^+$ for ^{138}Xe [16].

We perform the shell model calculations in the m–scheme. It is useful to replace the standard two–body Hamiltonian by the modified one

$$H = H + \alpha[\hat{\mathbf{J}}^2 - J(J+1)] \quad , \qquad (5)$$

Table 1. Effective single particle energies in MeV.

Protons		Neutrons	
$1g_{7/2}$	0.00	$2f_{7/2}$	0.00
$2d_{5/2}$	0.96	$3p_{3/2}$	0.85
$2d_{3/2}$	2.71	$1h_{9/2}$	1.56
$1h_{11/2}$	2.80	$3p_{1/2}$	1.66
$3s_{1/2}$	3.50	$2f_{5/2}$	2.00
		$1i_{13/2}$	2.11

where α is a positive constant. Due to the additional term, the states with total spin different from J are pushed up in energy for a sufficiently large value of α. Thus, the diagonalization yields only the low-lying states of a given spin J.

For ensuring the convergence of the results we determine a series of small positive values $\{\epsilon_1 > \epsilon_2 > \ldots > \epsilon_m\}$ and used them as a sampling criterion in Eq. (4). To each value of ϵ corresponds an unique number of configuration states which determines the dimension of the Hamiltonian matrix to be diagonalized.

The shell model problem for ^{140}Xe does not need a severe truncation of the configuration space for any J^π value, but we will use the importance sampling to restrict the size of the Hamiltonian. In [10], the behavior of the energies of the lowest $J^\pi = 0^+$ states and the value of the $B(E2;0_1^+ \rightarrow 2_1^+)$ as functions of the size of the Hamiltonian matrix is demonstrated. The efficiency of the method is observed also for the low lying states of ^{140}Xe. In Figs. 1 and 2 we present the convergence of the eigenvalues of the modified Hamiltonian for high-spin states $J^\pi = 10^+$ and $J^\pi = 12^+$ as a function of the dimension of the Hamiltonian matrix n normalized to the total size of the configuration space N.

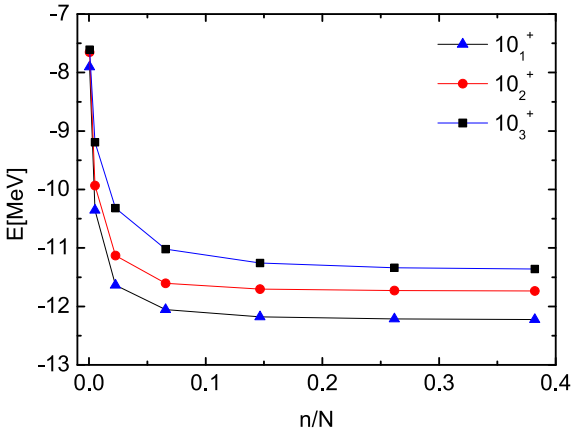

Figure 1. Convergence of the eigenvalues of the modified Hamiltonian for the lowest $J^\pi = 10^+$ states in ^{140}Xe.

It is seen that the properties of the important sampling do not depend on the spin of the modified Hamiltonian (5). The convergence of the eigenvalues of the Hamiltonian is

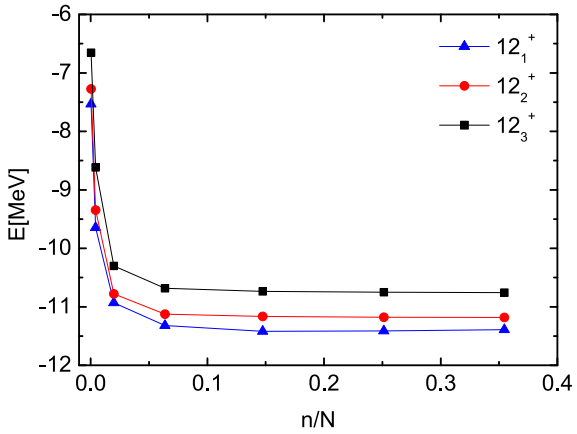

Figure 2. Convergence of the eigenvalues of the modified Hamiltonian for the lowest $J^\pi = 12^+$ states in ^{140}Xe.

reached for less then 10% of the size of the Hamiltonian. One should mention that for large configuration space the conversions is reached even for much smaller fraction of it. As demonstrated in [17] for ^{98}Zr high accuracy of the solution of the eigenvalue problem is obtained for $n/N \sim 10^{-5}$.

4 Results

In this section we will discuss the spectroscopic properties of the yrast line of ^{140}Xe up to $J^\pi = 12^+$. The energy spectrum of ^{140}Xe is presented in Fig.3. It is compared with the experimental data [18] and the previous shell model calculations [7].

The present results for the low-lying states slightly improve the agreement with the experimental data [16] compared with the previous calculations [7]. The calculated values of excitation energies of the $J^\pi = 10^+$ and $J^\pi = 12^+$ states are reproduced not so accurately but one should bear in mind, that the parameters of the problem we use, are fitted to the ^{138}Xe spectrum.

The experimental data on the transition rates for the xenon isotopes are too scarce for a detailed analysis of the nuclear structure. Table 2 shows the comparison between the experimental B(E2, $J_i \to J_f$) transition rates [18] with the two sets of theoretical shell model calculations. In both sets the adopted proton and neutron effective charges are $e_\pi = 1.6e$ and $e_\nu = 0.7e$ respectively. It is seen that the theoretical results follow the trend of the experimental data, although they slightly overestimate them. We like to point out, however, that the B(E2) are very sensitive to the effective charges. If we reduced both e_π and e_ν values by a factor 0.9 we get B(E2) strengths considerably close to the experimental data (for instance B(E2, $2_1^+ \to 0_1^+$) =27.87, and B(E2, $4_1^+ \to 2_1^+$) =40.89).

As already discussed in [7] it is worth mentioning that the large B(E2, $4_1^+ \to 2_1^+$) value, observed experimentally and reproduced fairy good by the calculations, suggests a large quadrupole deformation of the yrast 4^+ state.

It is also interesting to study the low-lying non-yrast $J^\pi = 2^+$ states, although only the experimental value just

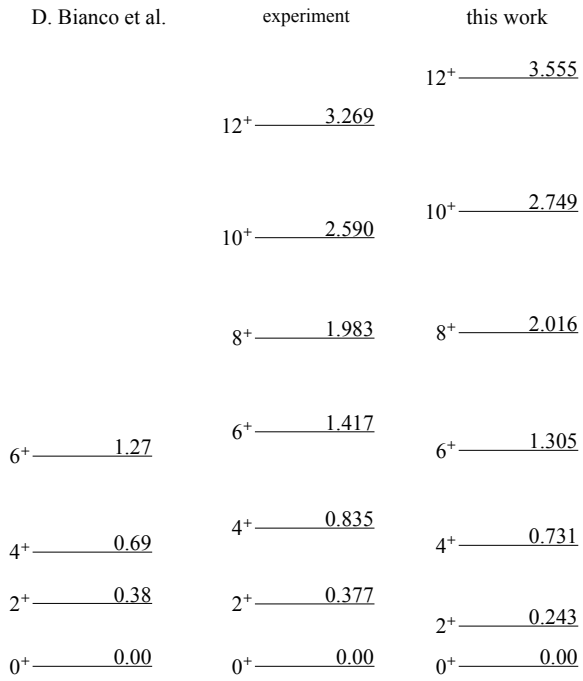

Figure 3. Low energy spectrum of ^{140}Xe, compared with the experimental data from ref. [18] and the previous shell model calculations [7].

Table 2. Experimental and theoretical B(E2, $J_i \to J_f$) values in [W.u.].

$J_i \to J_f$	Exp [18]	SM [7]	this work
$2_1^+ \to 0_1^+$	24.08 ± 4.63	30.93	34.41
$4_1^+ \to 2_1^+$	40 (8)	46.00	50.48
$6_1^+ \to 4_1^+$	> 22	48.44	52.98
$8_1^+ \to 6_1^+$			49.14
$10_1^+ \to 8_1^+$			56.07
$12_1^+ \to 10_1^+$			45.82

for the first 2^+ excitation energy is available [18]. The spectrum of the $J^\pi = 2_i^+, i = 1-6$ states is shown in Fig. 4 and compared with the results from [7]. It is seen that there are significant differences in the excitation energies of the states higher then 2_3^+. The properties of the first excited $J^\pi = 2^+$ states in both sets in the shell model calculations are fairy close. The excitation energies and the $E2$ and $M1$ transitions strength in ^{140}Xe do not differ significantly as well as seen in Table 3.

5 Conclusions

The present study has shown that the importance sampling algorithm can be extended successfully to high spin states of the neutron rich xenon isotop ^{140}Xe. It is able to reproduce the properties of the excited states of the yrast line up to $J^\pi = 12^+$ as well as the available experimental $E2$ transition rate. The present work confirms that the low and high spin spectra of the nuclei in the region around ^{132}Sn

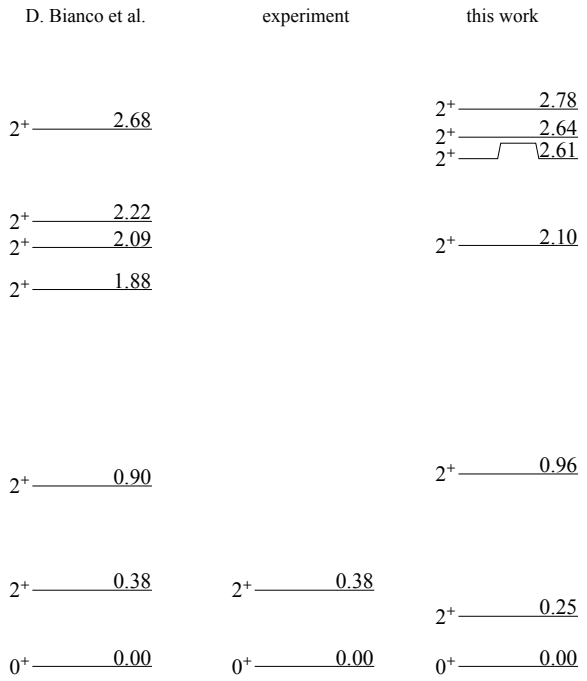

Figure 4. Low energy spectrum of ^{140}Xe, compared with the experimental data [18] and the previous shell model calculations [7].

Table 3. $E2$ and $M1$ transitions strength in ^{140}Xe.

$J_i \to J_f$	SM [7]	this work
B(E2)(W.u.)		
$2_1^+ \to 0_1^+$	30.93	34.41
$2_2^+ \to 0_1^+$	0.94	2.06
$2_2^+ \to 2_1^+$	5.79	4.41
B(M1)(W.u.)		
$2_2^+ \to 2_1^+$	0.00	0.02

can be studied simultaneously using the importance sampling algorithm and the same parameters of the large scale shell model problem.

This work is partly supported by the DFNI-T02/19 grant of the Bulgarian Science Fond. This financial support is gratefully acknowledged.

References

[1] C. Bauer *et al.*, Phys. Rev. C **88**, 021302(R) (2013) and references therein.
[2] N. Lo Iudice, V.Yu. Ponomarev, C. Stoyanov, A.V. Sushkov, and V.V. Voronov, J. Phys. G: Nucl. Part. Phys. **39**, 043101 (2012)
[3] N. Shimizu, T. Otsuka, T. Mizusaki, and M. Honma, J. Phys. Conf. Series **49**, 178 (2006)
[4] K. Sieja, G. Martínez-Pinedo, L. Coquard, and N. Pietralla, Phys. Rev. C **80**, 054311 (2009)
[5] D. Bianco, F. Andreozzi, N. Lo Iudice, A. Porrino, and F. Knapp, Phys. Rev. C **85**, 034332 (2012)
[6] D. Bianco, N. Lo Iudice, F. Andreozzi, A. Porrino, and F. Knapp, Phys. Rev. C **86**, 044325 (2012)
[7] D. Bianco, N. Lo Iudice, F. Andreozzi, A. Porrino, and F. Knapp, Phys. Rev. C **88**, 024303 (2013)
[8] L.Y. Jia, H. Zhang, and Y.M. Zhao, Phys. Rev. C **75**, 034307 (2007)
[9] F. Andreozzi, A. Porrino and N. Lo Iudice, J. Phys. A **35**, L61 (2002)
[10] S.S. Dimitrova and N. Lo Iudice, J. Phys. Conf. Series, **1023**, 012015 (2018)
[11] F. Andreozzi, N. Lo Iudice and A. Porrino, J. Phys. G **29**, 2319 (2003)
[12] D. Bianco, F. Andreozzi, N. Lo Iudice, A. Porrino and F. Knapp, J. Phys. G: Nucl. Part. Phys. **38**, 025103 (2011)
[13] D. Bianco, F. Andreozzi, N. Lo Iudice, A. Porrino and S. Dimitrova, J. Phys. Conf. Series **205**, 12002 (2010)
[14] M. Hjorth-Jensen, T.T. Kuo, and E. Osnes, Phys. Rep. 261, 125 (1995)
[15] R. Machleidt, Phys. Rev. C **63**, 024001 (2001)
[16] Jun Chen, Nucl. Data Sheets **146**, 1 (2017)
[17] S.S. Dimitrova, D. Bianco, N. Lo Iudice, F. Andreozzi and A. Porrino, in *Nuclear Theory: Proc. 32nd Int. Workshop on Nuclear Theory* (Rila, Bulgaria, June 23-29, 2013), eds. A. Georgieva, N. Minkov, Heron Press, Sofia, p. 100, ISSN: 1313-2822.
[18] N. Nica, Nucl. Data Sheets, **108**, 1287 (2007)